Journal of
Polymer & Composites
https://journals.stmjournals.com/jopc

ISSN: 2321-2810 (Online)
ISSN: 2321-8525 (Print)
Volume 14, Special Issue 2, 2026
DOI (Journal): 10.37591/JoPC

Research JoPC

CFD Analysis of Double Diffusion Rotating Flow in a Cylindrical Annular MHD Braking System with Joules Heating and Dufour Effects

Subas Chandra Dash[1,*], Manoj Dubey[2]

Abstract

The present study has investigated Joules parameter significance on an axisymmetric whirling flow within a cylindrical annulus, specifically focusing on an MHD braking system. The cylindrical annulus braking system is packed lithium lid liquid (Pr = 0.015), aspect ratio = 2, and imposed to an axial heat and magnetic field. In this study, the modified MAC pressure correction method has been used to solve the mixed convection flow with double diffusion. In the presence of double diffusion condition, Dufour effect at positive buoyancy ratio has been investigated. The conclusions exhibit Isotherms, concentration, components of velocities owing to the occurrence robust axial magnetic field (Ha =30 and 100) and Dufour number (Df = 1 to 8) due to Joules number (J = 1 to 25). The presence of Joules parameter on average Nusselt and Sherwood magnitude has been visualized in the presence of MHD braking condition at positive buoyancy ratio. The presence of double diffusion causes the Dufour effect to boost the Joule heating parameter, leading to a drastic magnification of heat and mass convection within the MHD braking system, and the inverse is also true. With a tiny Joule heating parameter, the Dufour effect's impact on heat and mass convection was negligible.

Keywords: Double diffusion, Joules heating, Magneto-hydrodynamics, Liquid metal, Dufour effect

INTRODUCTION

Researchers have explored the challenges of double diffusion flow in several disciplines, including oceanography, metallurgy, and mantle convection (Huppert and Turner, [1]; Turner [2, 3]; Lister and Buffett [4]; Simitev [5]). In addition, it has been cleared that the Earth's core exists in a state of compositional buoyancy, distinguished by significant variations in temperature and concentrations of light elements, which influence molecular diffusivity (Braginsky and Roberts, 1995). Focusing on its practical applications, double diffusive conversion is gaining interest across various fields such as astrophysics, geology, biology, and chemical engineering Nimmo [6]. The double diffusion flow is significant due to its applications in cooling electronic equipment, building structures with multi -shield in nuclear reactors, producing crystal formation, float gas, aeration processes, chemical reactors and various other applications [7-12]. Granger [13] and Tsiverblit and Kit [14] discussed these uses.

Recently, various studies have been carried out on fluid flow dynamics in a cylindrical cavity with rotating walls. Examples of these rotating flows can be found in practical contexts such as rotational viscometry, centrifugal machinery, the transfer of high-temperature liquid metals, the growth of crystals from molten silicon using Czochralski pullers, and in geophysical systems, according to

*Author for Correspondence
Subas Chandra Dash

[1,2]Assistant professor (SG), Department of Mechanical Engineering, Jaypee University of Engineering and Technology, Guna, Madhya Pradesh, India

Received Date: September 16, 2025
Accepted Date: October 27, 2025
Published Date: April 29, 2026

Citation: Subas Chandra Dash, Manoj Dubey. Application of Natural and Synthetic Polymer-Based Disintegrants in the Design of Fast Dissolving Cefuroxime Axetil Tablet Composites. Journal of Polymer & Composites. 2026; 14(2): S1448–S1462p.

© STM Journals 2026. All Rights Reserved

Bessaïh *et al*. [15]. Bessah *et al*. [16] evaluated the reliability of a rotating flow with axisymmetric nature in a cylindrical enclosure filled with lithium lid liquid with an aspect ratio (AR = 2).

They have made a stability diagram for the critical Reynolds number with an increase in Hartmann number for different Richardson number. In the absence of magnetic field and heat flux, the rotating flow in cylindrical annulus has been discussed by Dash and Sigh [17].

A detailed analysis has been undertaken with a significant number of simulations to find the breakdown zones associated with one-vortex and two-vortex flows in steady lid-driven swirls motion within a cylindrical annular cavity. Due to the occurrence of axial temperature gradient the change in flow field in confined rotating flow have been discussed in Dash and Sigh [18,19,20] and Dash [21]. Convection heat flow with double diffusion in a revolving cylindrical annulus with tapering cap has been discussed in Simitev [22]. He has visualized how a minor contribution from compositional buoyancy alongside thermal buoyancy, or vice versa, can notably lower the critical Rayleigh number. The examination of the unsteady mixed convection flow with double diffusion, incorporating Soret and Dufour effects in a lid driven cavity has been investigated by Ghaffarpas and [23] where he inferred that the presence of extra heat diffusion and Dufour effect due to natural convection influence heat transfer by producing thermal eddies. Satheesh, *et al* [24] have discussed the impact of Joules parameter along with Soret Number in a mixed convection flow due to double-diffusive in a closed square cavity.

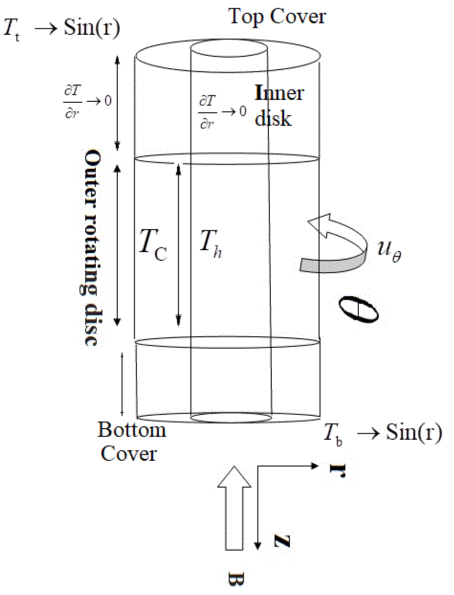

Figure 1. Diagram of revolving flow in cylindrical annular cavity MHD braking system, under the control of axial magnetic field and axial temperature gradient.

An analysis of how Joules heating and the Soret number impact double-diffusive mixed convection flow in a closed square chamber. The effect of Jouls heating on MHD flow in a vertical driven heat conducting square cavity have been discussed by Chatterjee [25]. The effect of Jouls heating on MHD flow in a vertical driven heat conducting square cavity have been discussed by Chatterjee [26].The effect of Lorentz force on Rotating confined MHD flow in cylindrical cavity have been discussed in Dash and Sigh [26, 27]. Related investigation have been carried out by Dash [28,29] where he has discussed the Joules parameter impact on rotating MHD flows within a cylindrical container filled with lithium lid liquid where MHD braking effects have been revealed. Sammouda and Gueraoui [30] analyzed convective flow considering double diffusion of Al2O3-water Nano-fluid inside a porous medium set within a cylindrical annular region formed by a pair of concentric cylinders; with areas of discrete heat in their 2021 publication. Recently Dash [31] have discussed the impact of double diffusion and Soret effect in a MHD braking system with an intensive magnetic field.

© STM Journals 2026. All Rights Reserved

ISSN: 2321-2810 (Online), ISSN: 2321-8525 (Print)

None of these above studies have investigated double diffusion MHD rotating flow with Joule heating effect parameters. Emphasizing the importance of a robust MHD force is essential, especially in scenarios involving MHD braking within electrically conducting fluid flows (like liquid metals) in nuclear reactor cooling systems, which are influenced by Joule heating and double diffusion caused by conducting walls and electric potential.The aforementioned literature review emphasizes an absence of studies on double diffusion caused by Joule heating within MHD braking systems, which has created an interest in investigation in the present research work.

NUMERICAL FORMULATION

This investigation looks into a cylindrical annulus cavity that is filled with an incompressible, viscous metallic fluid, characterized by a Prandtl number of 0.015, and influenced by both an axial magnetic field and an axial temperature gradient, Fig 1. Lithium-lead was picked for use as a working fluid in fusion reactor blankets because it serves as a tritium breeder and neutron multiplier, while also possessing beneficial thermo physical properties.

Prandt number(Pr) is not only a non- dimensional number but also property of fluid as well as fiction of temperature. With a low Prandtl number (Pr) of approximately 0.015, liquid lead-lithium exhibits a realistic characteristic of liquid metals, indicating that conduction, rather than convection, is the main method of heat transfer.

The upper and base cover, outer rotating disk and inner stationary disk surfaces barking system are equipped with material that have the ability to conduct both electricity and heat; whereas the rest portion of outer cylinder of the cavity is insulated. Due to the conducting material surfaces of this braking system, in this mathematical simulation heating by Joule parameter is considered.

Governing Equations

Throughout the study, all fluid characteristics retain their consistency, with the exception of density. Using the Boussinesq approximation, the density has been computed according to the equation; (1) and (2).

$$\rho = \rho_0[1 - \beta(T - T_C) - \beta_c(C - C_c)] \tag{1}$$

Where: $$\beta = -\frac{1}{\rho_0}\left(\frac{\partial \rho}{\partial T}\right)_{P,C}, \beta = -\left(\frac{\partial \rho}{\partial C}\right)_{P,T} \tag{2}$$

Considering the Boussinesq approximation, along with the combined effects of Soret number and heating due to Joule parameter, in the nonexistence of viscous dissipation; the non-dimensional governing equations are (Eqs. 3–7).

Mass Conservation:

$$\frac{1}{r}\frac{\partial(ru_z)}{\partial x} + \frac{\partial u_z}{\partial y} = 0 \tag{3}$$

Conservation of Momentum in radial direction:

$$\frac{\partial u_r}{\partial t} + \frac{1}{r}\frac{\partial(ru_r u_r)}{\partial r} + \frac{\partial(u_r u_z)}{\partial z} - \frac{u_\theta^2}{r} = -\frac{\partial p}{\partial r} + \frac{1}{\mathrm{Re}}\left[\frac{\partial}{\partial r}\left(\frac{1}{r}\frac{\partial r u_r}{\partial r} + \frac{\partial^2 u_z}{\partial z^2}\right) + \frac{Ha^2}{\mathrm{Re}}F_{lr}\right] \tag{4}$$

Conservation of Momentum in axial direction:

$$\frac{\partial u_y}{\partial t} + \frac{1}{r}\frac{\partial(ru_r u_z)}{\partial r} + \frac{\partial(u_z u_z)}{\partial z} = -\frac{\partial p}{\partial z} + \frac{1}{\mathrm{Re}}\left[\frac{1}{r}\frac{\partial}{\partial r}\left(r\frac{\partial r u_z}{\partial r}\right) + \frac{\partial^2 u_z}{\partial z^2}\right] + \frac{Ha^2}{\mathrm{Re}}F_{lz} + \mathrm{Ri} \times (T + NC) \tag{5}$$

Conservation of Momentum in Azimuthal direction:

$$\frac{\partial u_\theta}{\partial t} + \frac{1}{r}\frac{\partial(ru_r u_\theta)}{\partial r} + \frac{\partial(u_z u_\theta)}{\partial z} + \frac{u_r u_\theta}{r} = \frac{1}{\mathrm{Re}}\left[\frac{\partial}{\partial r}\left(r\frac{\partial r u_\theta}{\partial r}\right) + \frac{\partial^2 u_\theta}{\partial z^2}\right] + \frac{Ha^2}{\mathrm{Re}}F_{l\theta} \tag{6}$$

© STM Journals 2026. All Rights Reserved

Energy Equation:

$$\frac{\partial T}{\partial t}+\frac{1}{r}\frac{\partial(ru_rT)}{\partial r}+\frac{\partial(u_zT)}{\partial z}=\frac{1}{\mathrm{RePr}}\left[\frac{1}{r}\frac{\partial}{\partial r}\left(r\frac{\partial T}{\partial r}\right)+\frac{\partial^2 T}{\partial z^2}\right]+J\times\left[u_r^2+u_\theta^2\right]+\frac{Df}{\mathrm{Re}}\left(\frac{1}{r}\frac{\partial}{\partial r}\left(r\frac{\partial C}{\partial r}\right)+\frac{\partial^2 C}{\partial z^2}\right) \quad (7)$$

Concentration:

$$\frac{\partial C}{\partial t}+\frac{1}{r}\frac{\partial(ru_rC)}{\partial r}+\frac{\partial(u_zC)}{\partial z}=\frac{1}{\mathrm{Re}Sc}\left[\frac{1}{r}\frac{\partial}{\partial r}\left(r\frac{\partial C}{\partial r}\right)+\frac{\partial^2 C}{\partial z^2}\right]+\frac{Sr}{\mathrm{Re}}\left(\frac{1}{r}\frac{\partial}{\partial r}\left(r\frac{\partial T}{\partial r}\right)+\frac{\partial^2 T}{\partial z^2}\right) \quad (8)$$

Equation for Magnetic Flux: $\frac{1}{r}\frac{\partial}{\partial r}\left(r\frac{\partial \Phi}{\partial r}\right)+\frac{\partial^2\Phi}{\partial z^2}=\frac{u_\theta}{r}+\frac{\partial u_\theta}{\partial r}$ (9)

Where the equations for Lorentz forces are given as;
In radial direction $F_{lr}=-u_r$ (10-a), in axial direction $F_{lz}=-u_r$ (10-b) and in Azimuthal direction $F_{l\theta}=\frac{\partial\Phi}{\partial r}-u_\theta$ (10-c).`

Velocity, Temperature, Mass concretion and magnetic field Boundary Conditions:

On outer surface of inner vertical Brake Disk:

Top Portion: $r=0.1, 1.5\le \mathrm{z}\le 2.0, u_r=0, \mathrm{u}_\theta=0, \mathrm{u_z}=0, \frac{\partial \mathrm{T}}{\partial \mathrm{r}}=0, \frac{\partial \mathrm{c}}{\partial \mathrm{r}}=0, \frac{\partial\Phi}{\partial \mathrm{r}}=0$ (11-a)

Middle Portion: $r=0.1, 0.5\le \mathrm{z}\le 1.5, u_r=0, \mathrm{u}_\theta=0, \mathrm{u_z}=0, T=1.0, \frac{\partial \mathrm{c}}{\partial \mathrm{r}}=0, \frac{\partial\Phi}{\partial \mathrm{r}}=0$ (11-b)

Bottom Portion: $r=0.1, 0\le \mathrm{z}\le 0.5, u_r=0, \mathrm{u}_\theta=0, \mathrm{u_z}=0, \frac{\partial \mathrm{T}}{\partial \mathrm{r}}=0, \frac{\partial \mathrm{c}}{\partial \mathrm{r}}=0, \frac{\partial\Phi}{\partial \mathrm{r}}=0$ (11-c)

On inner surface of outer vertical Brake disk:

Top Portion: $r=1.0, 1.5\le \mathrm{z}\le 2.0, u_r=0, \mathrm{u}_\theta=0, \mathrm{u_z}=0, \frac{\partial \mathrm{T}}{\partial \mathrm{r}}=0, \frac{\partial \mathrm{c}}{\partial \mathrm{r}}=0, \frac{\partial\Phi}{\partial \mathrm{r}}=0$ (12-a)

Middle Portion: $r=1.0, 0.5\le \mathrm{z}\le 1.5, u_r=0, \mathrm{u}_\theta=\Omega\times \mathrm{r}, \mathrm{u_z}=0, T=0.0, \frac{\partial \mathrm{c}}{\partial \mathrm{r}}=0, \Phi=\frac{\mathrm{r}^2}{2}$ (12-b)

Bottom Portion: $r=1.0, 0\le \mathrm{z}\le 0.5, u_r=0, \mathrm{u}_\theta=0, \mathrm{u_z}=0, \frac{\partial \mathrm{T}}{\partial \mathrm{r}}=0, \frac{\partial \mathrm{c}}{\partial \mathrm{r}}=0, \frac{\partial\Phi}{\partial \mathrm{r}}=0$ (12-a)

On the bottom Cover:

$$z=0.0.1\le \mathrm{r}\le 1.0, u_r=0, \mathrm{u}_\theta=0, \mathrm{u_z}=0, T_\mathrm{b}=\mathrm{Sin(r)}, \frac{\partial \mathrm{c}}{\partial \mathrm{z}}=0, \frac{\partial\Phi}{\partial \mathrm{z}}=0 \quad (13)$$

On the Top Cover:

$$z=\mathrm{h}, 0.1\le \mathrm{r}\le 1.0, u_r=0, \mathrm{u}_\theta=0, \mathrm{u_z}=0, T_\mathrm{T}=\mathrm{Sin(r)}, \frac{\partial \mathrm{c}}{\partial \mathrm{z}}=0, =0, \frac{\partial\Phi}{\partial \mathrm{z}}=0 \quad (14)$$

$$\mathrm{Nu}=-\left(\frac{\partial T}{\partial r}\right)_{z=0} \quad (12)$$

$$\mathrm{Nu_{avg}}=-\frac{1}{R}\int \mathrm{Nudr} \quad (15)$$

$$\mathrm{Sh}=-\left(\frac{\partial c}{\partial r}\right)_{z=0} \quad (14)$$

$$\mathrm{Sh_{avg}}=-\frac{1}{R}\int \mathrm{Shdr} \quad (16)$$

The Solution Procedure

In order to get the solution of the incompressible Navier-Stoke equation, the current numerical method employs the modified MAC approach, which are described in detail in a study by Chorin [32] and Peyter and Taylor [33]. Also my preceding articles, Dash and Singh [26] and Dash and Singh [27], have been discussed the convergence criteria in detail. To solve the momentum equations for radial and axial directions in the meridional plane, a pressure correction method is employed. The resolution

© STM Journals 2026. All Rights Reserved

between the nth time level and the (n+1)th time level is handled explicitly, yielding a velocity field that may or may not meet the mass conservation (i.e. equation for continuity) requirements. This challenge is solved by utilizing a pressure correction approach for each cell, which corrects the pressure and velocity components in a stepwise manner, guaranteeing that the final pressure distribution results in a zero velocity divergence in every cell. This process will repeat until the divergence of velocity in every cell is below the designated maximum limit, established as 0.000001 for the current research.

The steps required to tackle the governing equations, along with the concentration ratio equation relevant to double diffusion flow, have been discussed in my current publication Dash [31, 2025].

Code validation: The findings of present simulation at the parameters of Reynolds number Re = 900, Prandtl number (Pr = 0.015), Richardson number Ri = 1 and Hartmann number Ha = 5 for aspect ratio AR = 2.0, as align closely with those of [Mahfoud and Bessaih, 2012a, 16] demonstrated in Fig 2.

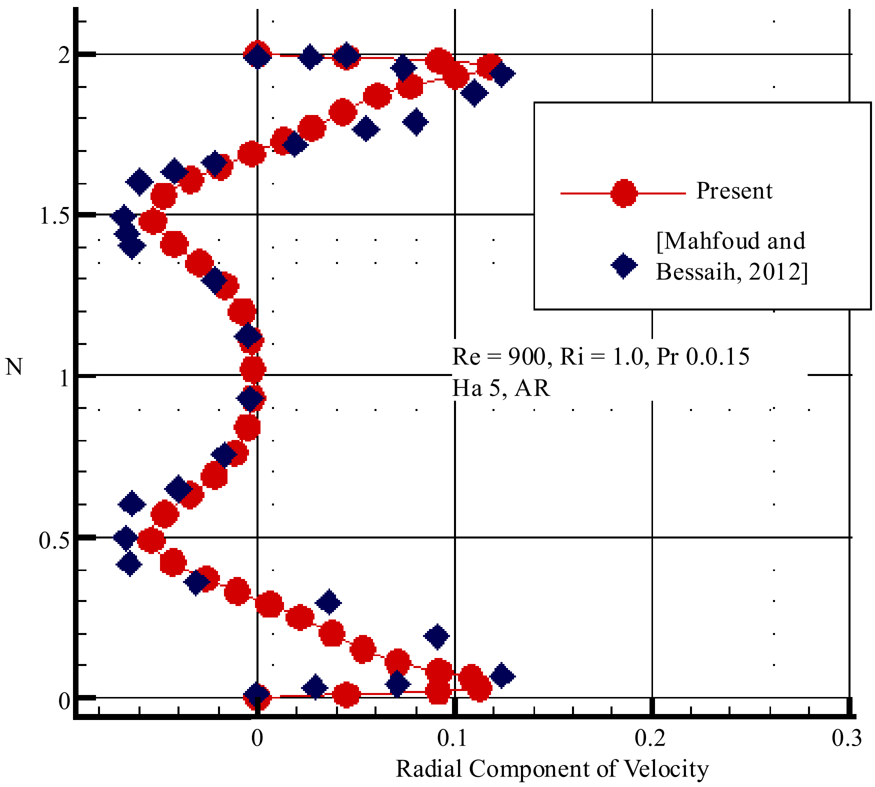

Figure 2. (a) Ri= 1, Re = 900, Pr =0.015, Sr = 0, Df = 0, Ha= 5 and AR =2.0.

The stability of rotating flow in a confined cylindrical cavity has been experimentally investigated by Escudier [34] depends upon aspect ratio as well as Reynolds number in absence of heat transfer and magnet force. *My previous investigation Dash and Sigh [27] shows the influence of MHD on stability in Aspect ratio-Reynolds number zone. At AR =2, Re = 1000, the flow is steady. In the present investigation, the influence of double diffusion, Joules heating due to a strong magnetic field has been further considered.* The selection of AR = 2 is often defended on the grounds that it reflects a transitional regime showcasing sophisticated, three-dimensional flow phenomena, such as vortex breakdown and different instabilities.

The grid independence test has been carried out for three different grids i.e. 100X200, 150X300 and 200X 400 having aspect ratio AR =1.0. It has been visualized from Fig (2-b) (i) and (ii) that the change in magnitude of Azimuthal and radial components of velocities are insignificantly change due to grid independence test

© STM Journals 2026. All Rights Reserved

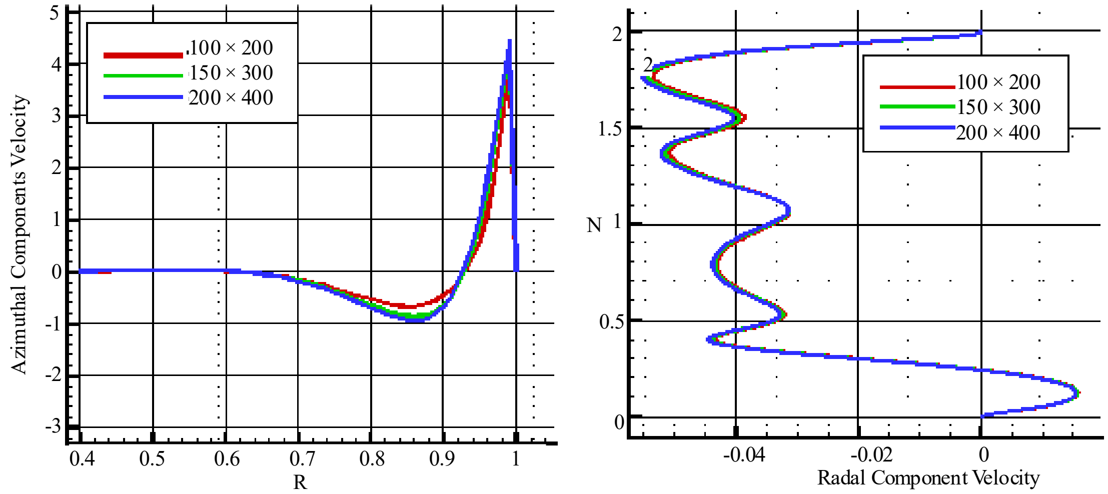

Figure 2. (b) At Re = 1000, Ha = 25, Ri=0.015, Pr= 0.015, Sc=5.0, NC= 2, Sr =0.25, Df =7.0, J= 1.0 at different grids.

RESULTS AND DISCUSSION

The unsteady flow field due to the presence strong joules heating at higher Dufour effect at Re = 1000, Pr =0.015, Ri =0.015 at lower Hartmann strength Ha =30 within the MHD braking system shown in Fig 3. Due to intensified Joules effect the developed unsteady flow field can be seen all three components of velocities.

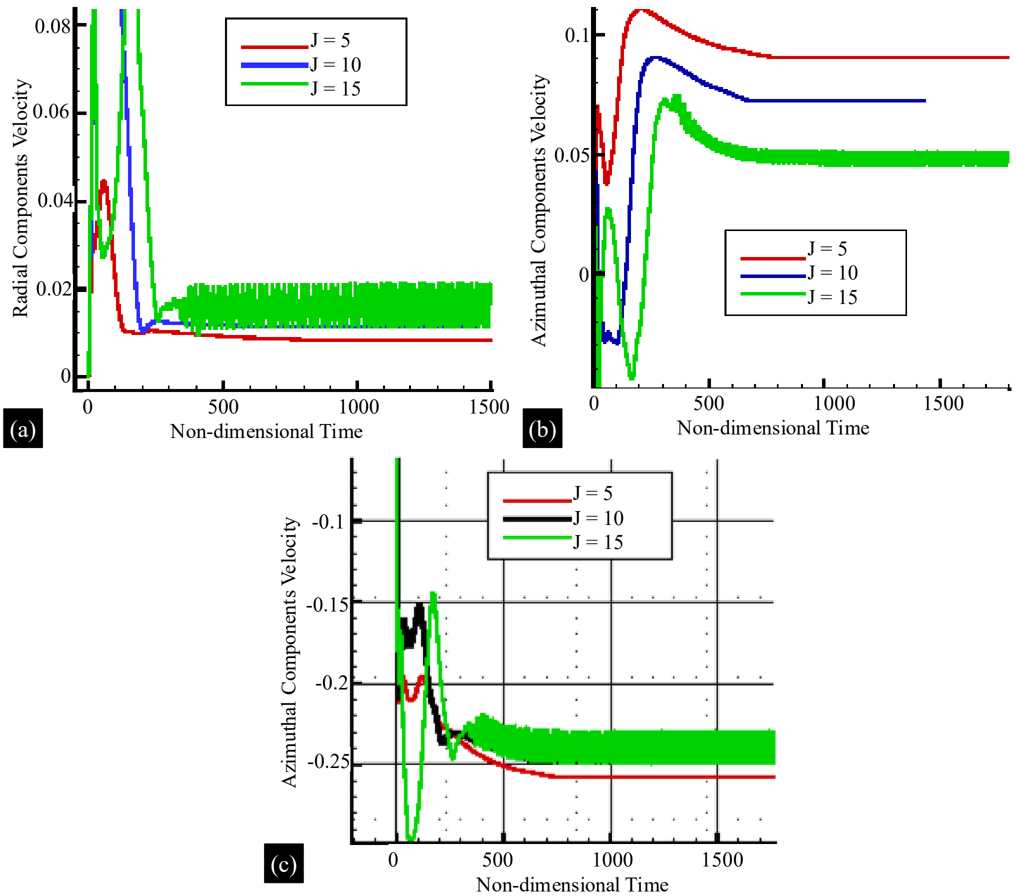

Figure 3. Effects of Joules heating on double diffusion fluid: Re = 1000, Ha = 25, Ri=0.015, Pr= 0.015, Sc=5.0, NC= 2, Sr =0.25, Df =7.0 at different Joules heating parameters.

The profiles of velocity components presented in Fig 4 demonstrate how the Joules heating parameter impacts the flow field in the MHD braking system. It can be observed that as the Joules heating parameters in (J = 5 to J = 15) increase, the increase in the magnitude of both the radial and azimuthal components of velocity becomes insignificant when compared to the axial component of velocity.

Because of this axial magnetic field strength existence, the Lorentz fore in along the axial direction disappears and it has no controlling effects on flow field on the other hand the increasing Joules heating parameter develops more bouncy effects both of heat and mass. Hence, the axial component velocity enhances predominantly with increasing Joules heating parameter, Fig 4 (b). Fig 5 shows the stream contours for flow filed within the MHD braking system at different Dufour number.

It indicates that maximum velocity induced vicinity to the rotating disc of the braking system and diminishes radially. However, the increasing Dufour effect reduces the Azimuthal velocity gradient in radial direction. Fig 6 shows the stream contours i.e. the fluid flow direction in meridional plane in order to understand the secondary flow pattern within the MHD braking sysytem. The fluid flow have two circulation in this plane one is upper positive and lower negative at J = 15. The contours of the concretion ratio shown in Fig 7 (a) to (d) demonstrate that the highest level of concretion occurs close to the innermost stationary hot disc because of fluid build-up.

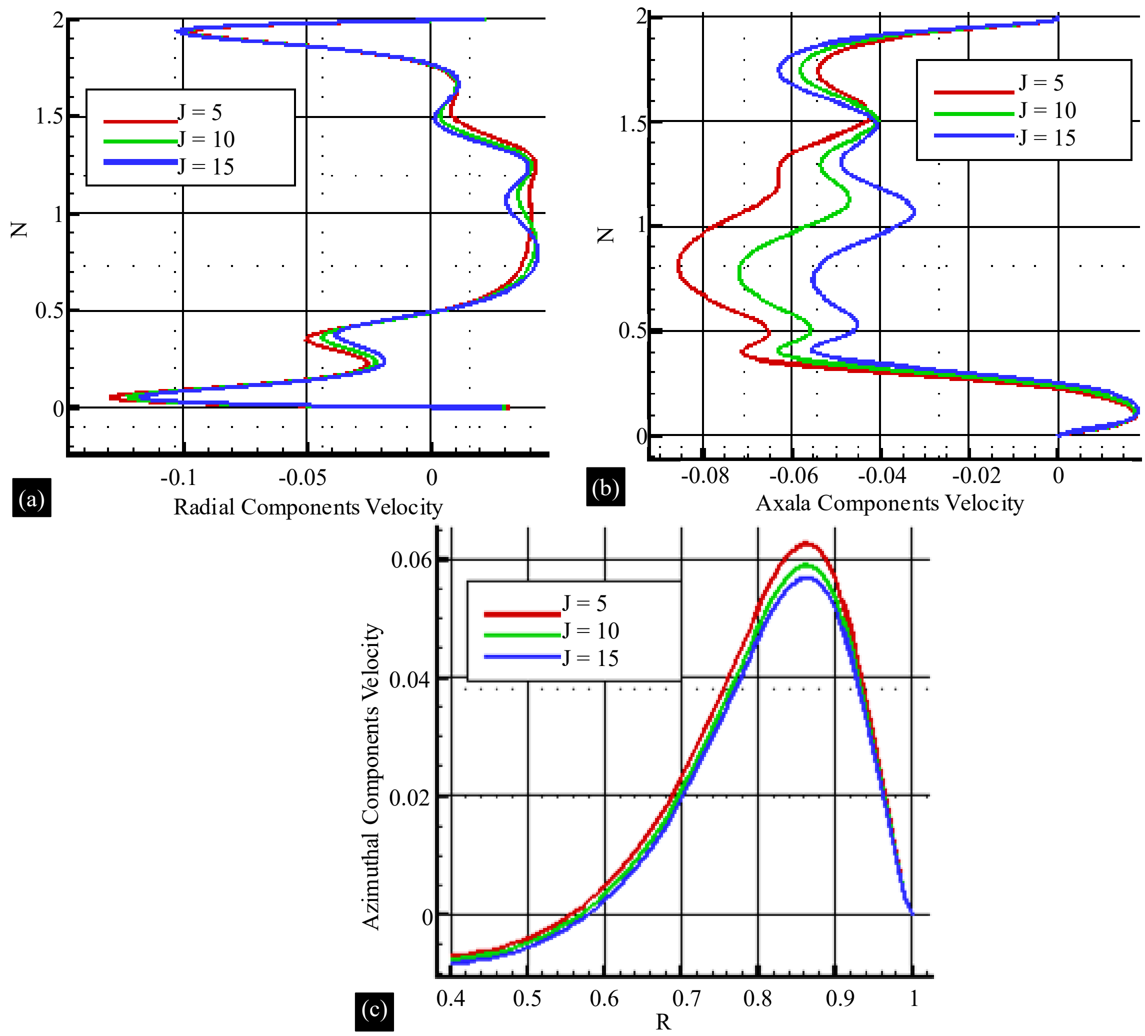

Figure 4. Joules heating parameters effects on velocity profiles (a) Radial components of velocity at r = 0.8 (b) Axial Components of Velocity at r =0.8 (c) Azimuthal components at Z = 0.5: Re = 1000, Ha = 100, Ri=0.015, Pr= 0.015, Sc=5.0, NC= 2, Sr =0.25 at different Dufour number.

© STM Journals 2026. All Rights Reserved

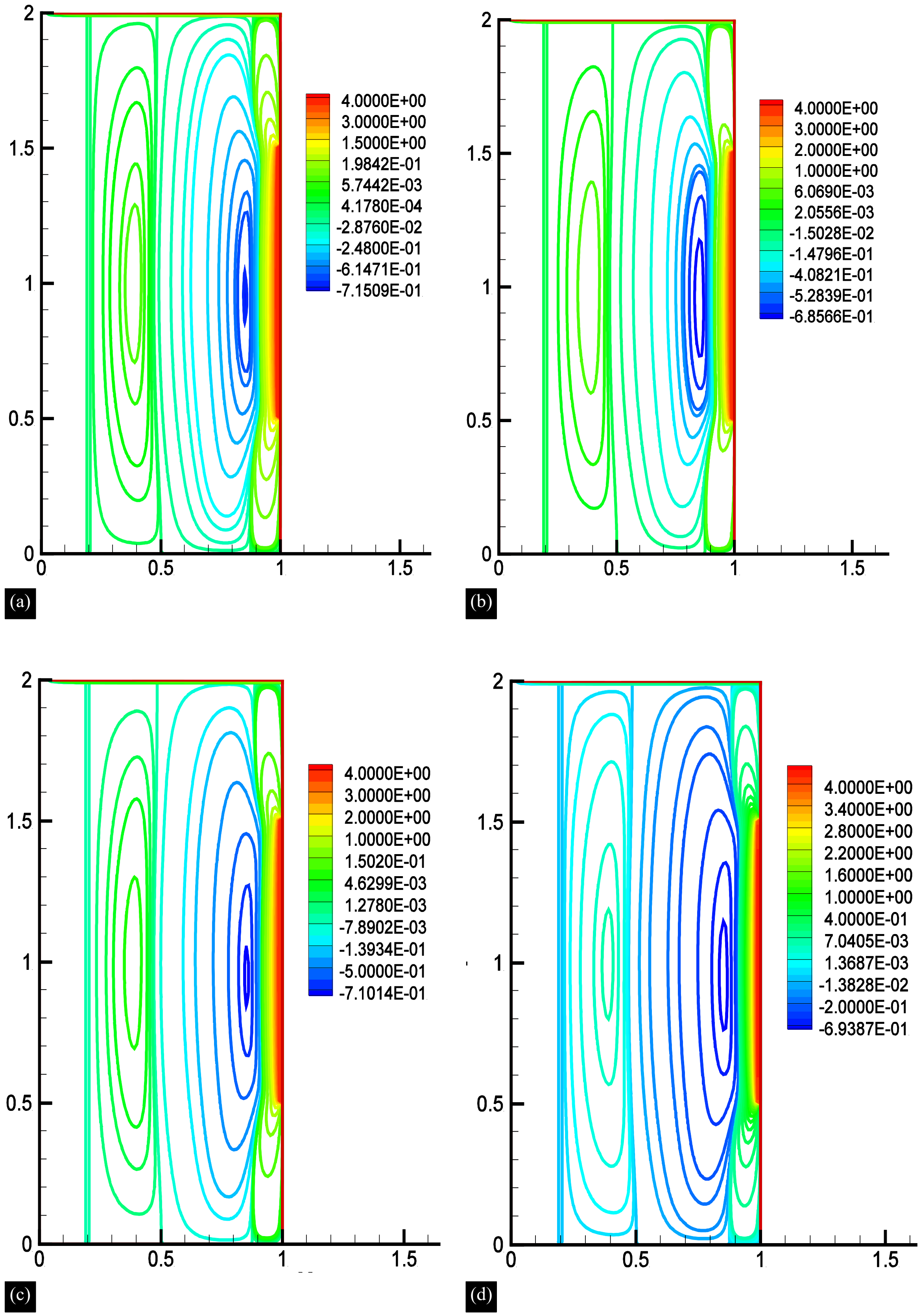

Figure 5. Azimuthal velocity contours: Re = 1000, Ha = 100, Ri=0.015, Pr= 0.015, Sc=5.0, NC= 2, Sr =0.25 at different Dufour number.

© STM Journals 2026. All Rights Reserved

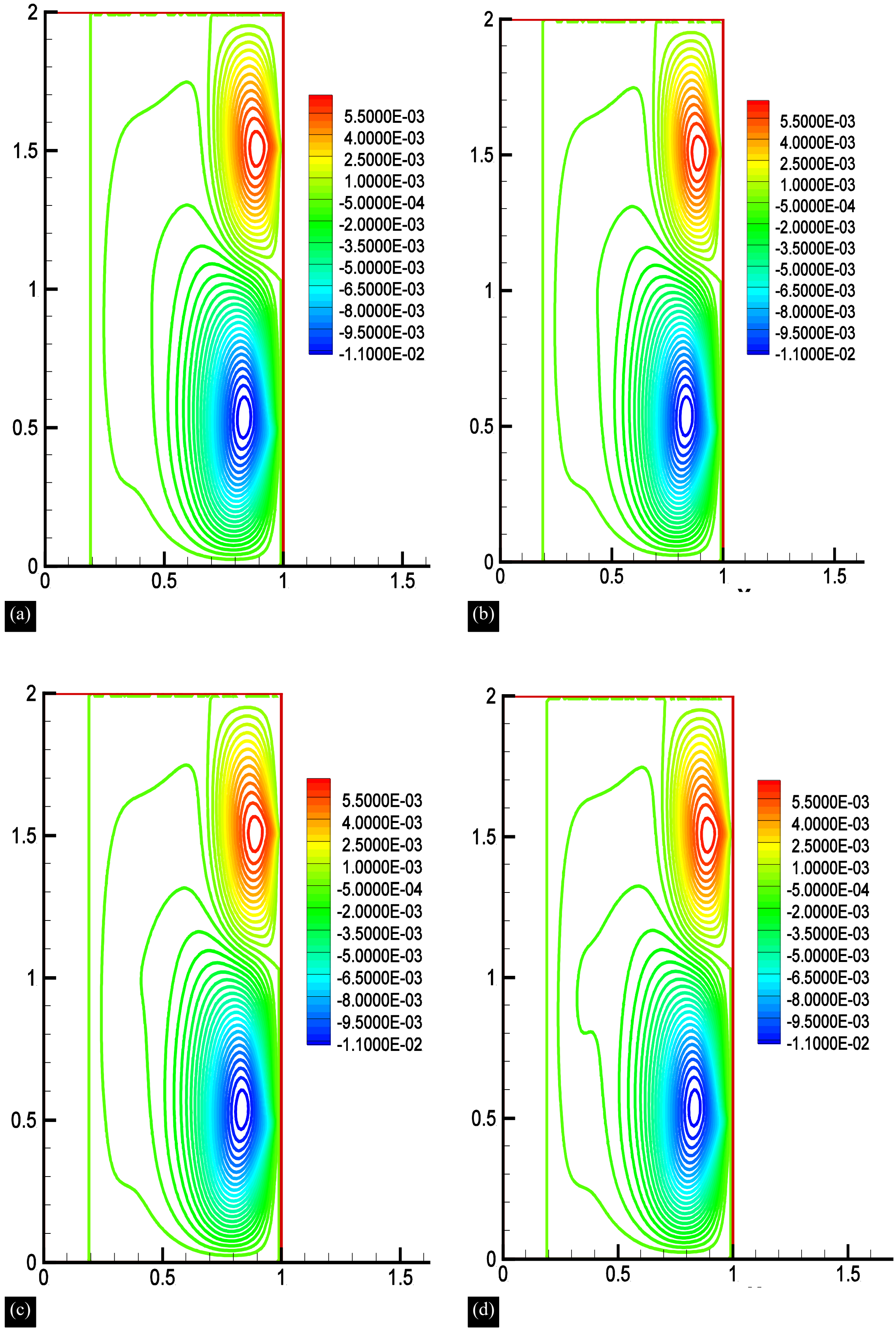

Figure 6. Stream line contours: Re = 1000, Ha = 100, Ri=0.015, Pr= 0.015, Sc=5.0, NC= 2, Sr =0.25 at different Dufour number.

© STM Journals 2026. All Rights Reserved

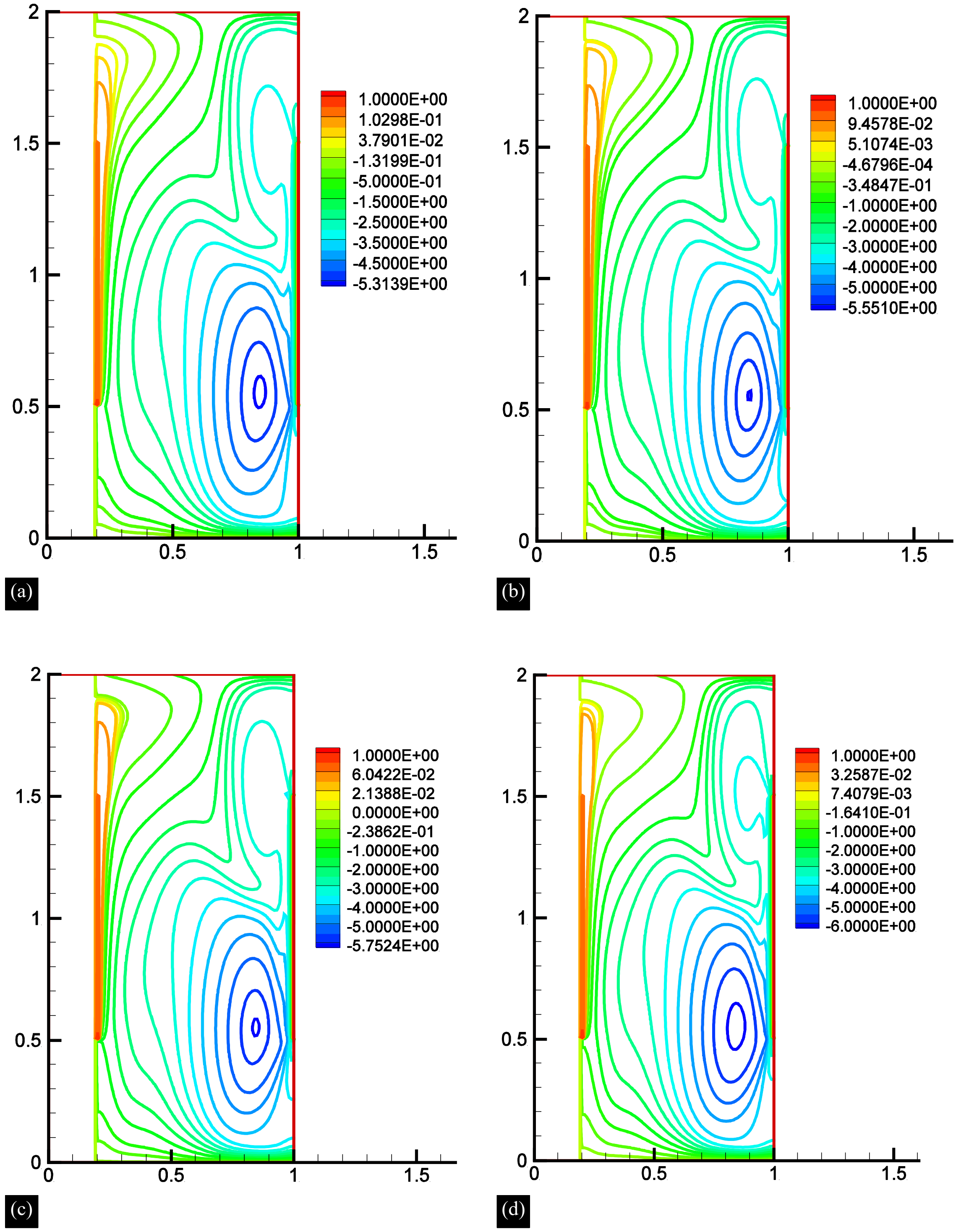

Figure 7. Concentration ratio contours: Re = 1000, Ha = 100, Ri=0.015, Pr= 0.015, Sc=5.0, NC= 2, Sr =0.25 at different Dufour number.

The cumulative consequence of Joule heating and the Dufour effect are illustrated in the numerical evaluation of the average Nusselt number (Nu) and Swearword number presented in Figures 8 to 10. It has been envisaged that average Nusselt number near inner disc increase both Joules heating parameter and Dufour effect are responsible for enhancing heat rate. However, near inner disc of braking system is magnitude drastically diminutive in comparison to vicinity of outer disc.

© STM Journals 2026. All Rights Reserved

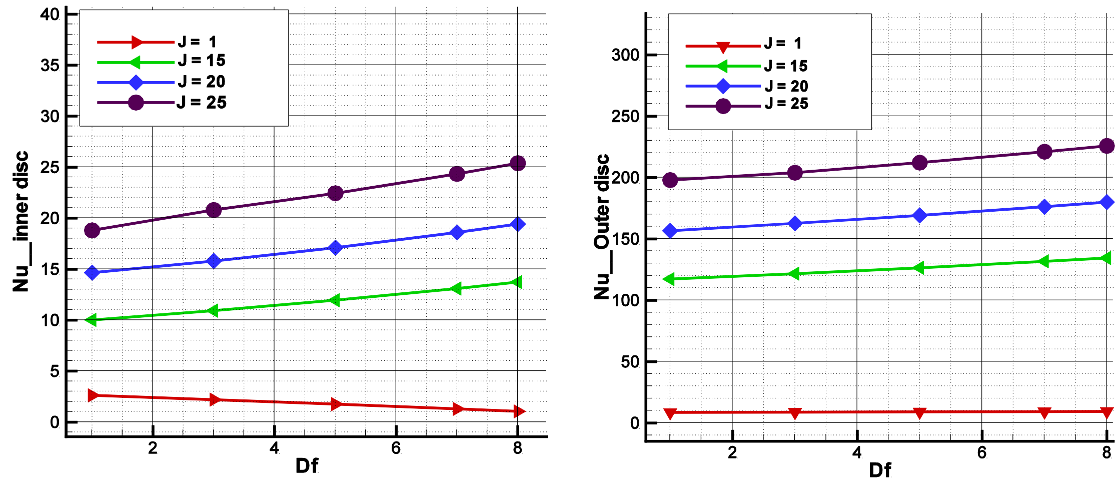

(a) (b)

Figure 8. Dufour effect in the existence of Joules parameter on Nusselt number (a) Near inner stationary disck (b) Outer rotating disc in the occurrence sturdy Magnetic field Ha =100. At Re = 1000, Ha = 150, Ri=0.015, Pr= 0.015, Sc=5.0, NC= 2, Sr =0.25

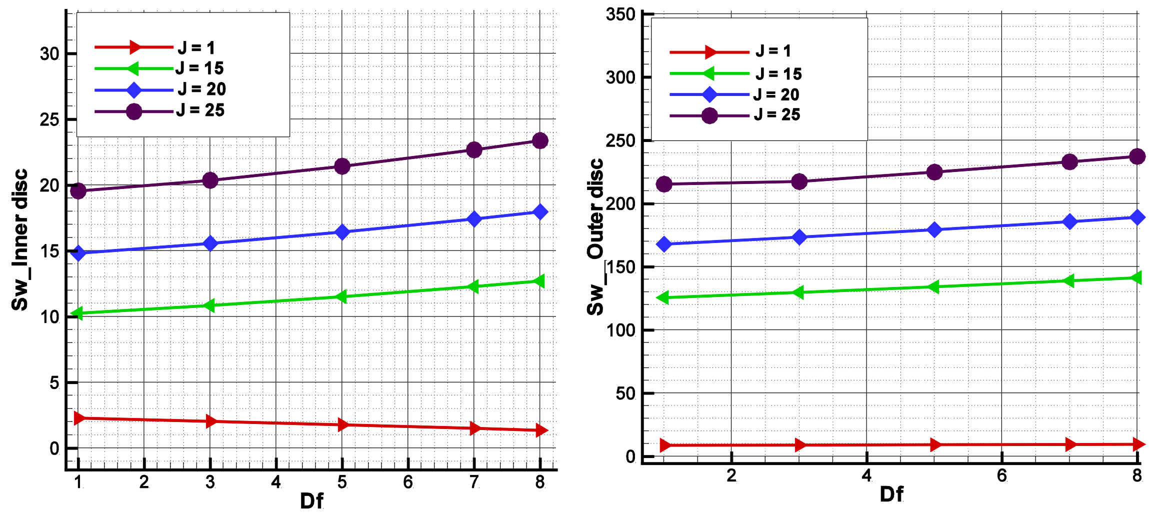

(a) (b)

Figure 9. Dufour effect in the occurrence of Joules parameter on Concentration ratio (Sherwood number) (a) Near inner stationary disck (b) Outer rotating disc in the occurrence sturdy Magnetic field Ha =100. At Re = 1000, Ha = 100, Ri=0.015, Pr= 0.015, Sc=5.0, NC= 2, Sr =0.25

The average Sherwood outcomes indicate its increasing presence in both the inner and outer discs of the braking system, as shown in Fig 7(a) and Fig 7(b). In the vicinity of the rotating disc of the MHD baking system, mass convection is highly prevalent relatives to the area near the inner stationary disc. Both the average Nusselt number (Nu) and Swearword number exhibit comparable trends, indicating that as the Joules heating parameter and Dufour effects escalate at Ha = 100, mass convection and heat rates also increase.

Figure 8 illustrates the impact of Joules heating and the Dufour number on heat rate and mass convection in scenarios of strong MHD braking (Ha = 100) compared to weaker magnetic field influences (Ha = 30). Figures 8 (a) and (b) illustrate the average Nusselt number, while Figures 8 (c) and (d) show the average Sherwood number. It has been shown that the presence of MHD braking leads

© STM Journals 2026. All Rights Reserved

to a reduction in heat and mass flow rates. This can be further visualized in Fig 9 and Fig 10. Fig 10 shows Dufour effects in the presence of strong magnetic filed in comparison to squat magnetic field.

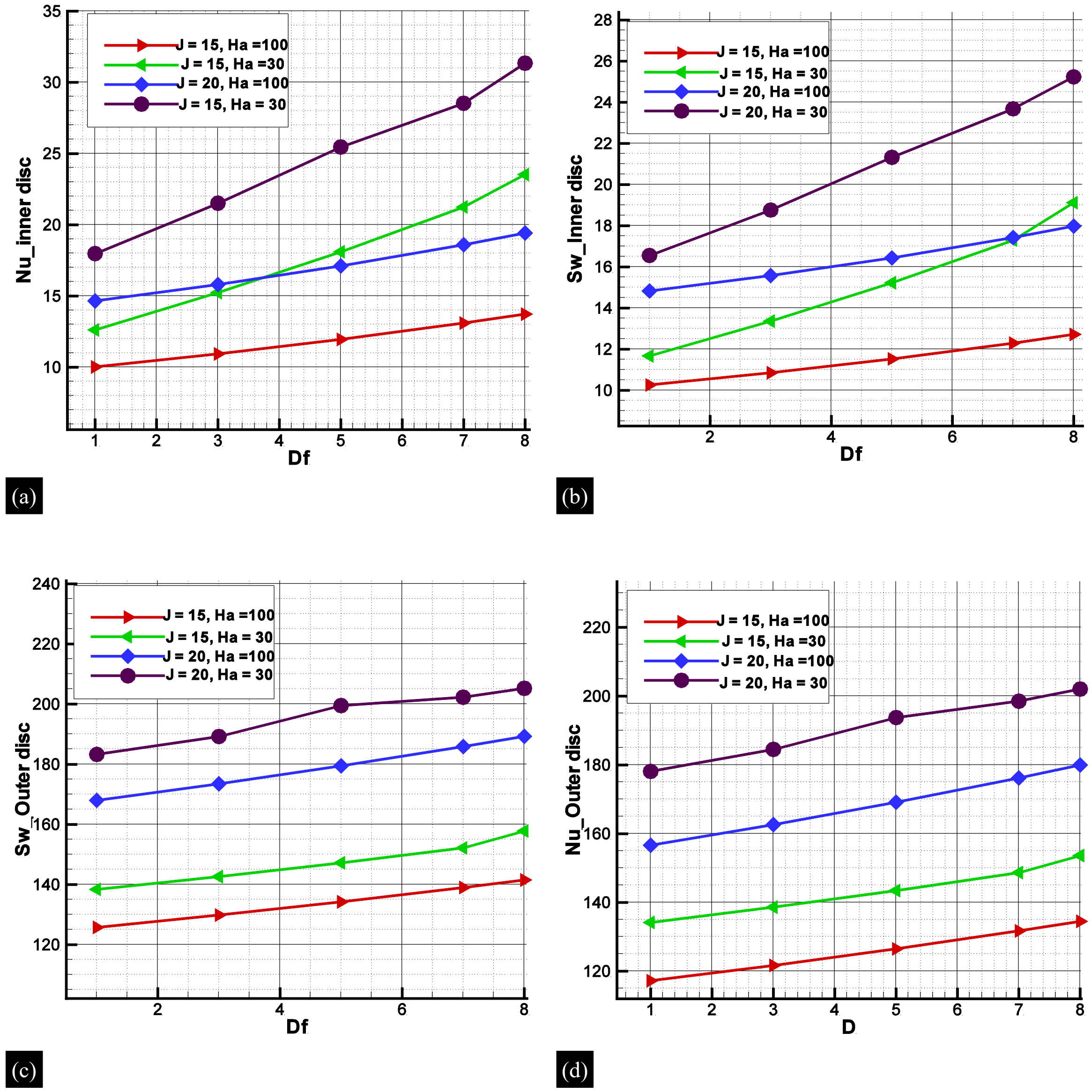

Figure10. Effects of Dufour number in the existence of Joules parameter on concentration ratio (Sherwood number) (a) Near inner stationary disc (b) Outer rotating disc. At Re = 1000, Ha = 100, Ri=0.015, Pr= 0.015, Sc=5.0, NC= 2, Sr =0.25. (At Ha =30 and Ha =100).

ABBREVIATIONS AND NOMENCLATURE

Nomenclature: AR - Aspect ratio = H/R B - Magnetic Field [kg/s3A] Df- Dufour parameter H - Height of cylinder [m] J- Joules heating parameter N- Positive bouncy ratio p- pressure [dimensionless] Sc- Schmitt number	u_r, u_θ, u_z - radial, azimuhal and axial velocity components [dimensionless] R - radius t- Non-dimensional time Φ - electric potential [dimensionless] Φ^* - electric potential	$Fl_\theta = \frac{\partial \Phi}{\partial r} - u_\theta\, Ha = BR\sqrt{\frac{\sigma}{\mu}}$ - Hartmann number $N = \frac{Ha^2}{\mathrm{Re}}$ Interaction parameter $\mathrm{Re} = \frac{R^2\Omega}{v}$ Reynolds Number $\Phi = \frac{\Phi^*}{(\Omega R^2 B)}$

© STM Journals 2026. All Rights Reserved

Sr- Soret number r, z, θ- coordinates in radial, axial and Azimuthal; direction [non-dimensional]	ν - kinematic viscosity [m^2/s] Ω - invariable angular velocity of outer disc[rad/s] σ - conductivity for electricity, μ - dynamic viscosity and $Fl_r = -u_r, Fl_y = 0$ Fl_r, Fl_y and - the Lorentz Fl_θ forces in radial, axial and azimuthal direction	

CONCLUSIONS

An investigation of double diffusive rotating flow within a cylindrical annular MHD braking system has been carried out at Re = 1000, Ha = 100, Ri = 0.015, Pr = 0.015, Sc = 5.0, and Sr = 0.25, focusing on a positive buoyancy ratio (N = 2) with Ha = 30 and Ha = 100. The flow has been analyzed using a range of Dufour parameters (DF = 1 to 8), while also considering a broad spectrum of Joules heating parameters (J = 1 to 20).

- It has been observed that at higher Joules heating effect the flow becomes unsteady and this instability vanishes in the existence of sturdy magnetic field and flow speed brakes.
- This indicates the existence of sturdy magnetic field restrains the stream of fluid in radial direction significantly and maximum mass concentration at midpoint of inner stationary disc.
- It is evident that maximum heat and mass convection occurs close to the rotating disc; however it approaches its minimum value near inner stationary disc. At Df = 8, J =25 , Near outer rotating disc the magnitude of Nu_{Oavg}= 232.378 and Sw_{Oavg} = 229.765 and near inner disc Nu_{Oavg}= 25.318 and Sw_{Oavg} = 23.576.
- Due to the double diffusion condition Dufour effect enhance Joules heating parameter and both the heat and mass convection within the MHD braking system magnifies drastically and vice versa. At diminutive Joule heating parameter J = 1, the Dufour effect has influenced the heat and mass convection insignificantly.

However, as the Joules heating parameters increases within a double diffusion the Dufour effect severely affects the heat and mass convection.

- This Dufour parameter along with Joules heating effects can be interpreted from Sherwood and Nusselt number magnitudes vicinity to the stationary and rotating disc of MHD braking system.

The interpretation of the changing Nusselt number suggests a boosted heat transfer rate, indicating that convection heat flow intensifies with its increase. On the other hand, the heightened Sherwood numbers indicate an increase in mass convection that corresponds to the observed heat transfer patterns.

Acknowledgement: We would like to acknowledge Dr Amiya Kumar Sahoo, faculty of Mechanical Engineering Department of Jaypee University of Engineering and Technology, Guna for his moral and technical support for this research work.

DECLARATION OF INTEREST

The authors declare that there is no conflict of interest regarding the publication of this manuscript.

REFERENCES:

1. Huppert H, Turner J S. Double-diffusive convection. *J. Fluid Mech*. 1981; 106, 299–329.
2. Turner J. Double-diffusive phenomena. *Annu Rev. Fluid Mech*. 1974 Jan;6(1):37-54.
3. Turner JS. Multicomponent convection. *Annu Rev. Fluid Mech*. 1985;17:11-44.

4. Lister JR, Buffett BA. The strength and efficiency of thermal and compositional convection in the geodynamo. *Phys. Earth Planet. Inter.*1995 Sep 1;91(1-3):17-30.
5. Simitev RD. Double-diffusive convection in a rotating cylindrical annulus with conical caps. *Phys. Earth Planet. Inter*. 2011 Jun 1;186(3-4):183-90.
6. Nimmo F. Enegretics of the core. In: Schubert, G. (Ed.).*Treatise on Geophysics*. 2007; 8: 31–65.
7. Braginsky SI, Roberts PH. Equations governing convection in Earth's core and the geodynamo. *GAFD*. 1995 Aug 1;79(1-4):1-97.
8. Schmitt RW. Double diffusion in oceanography. *Annu. Rev. Fluid Mech*.1994 Jan 1;26(1):255-85.
9. El Ayachi R, Raji A, Hasnaoui M, Abdelbaki A, Naïmi M. Resonance of double-diffusive convection in a porous medium heated with a sinusoidal exciting temperature. *J. Appl. Fluid Mech*. 2012; 1;3(2):43-52.
10. Bose PK, Sen D, Panua R, Das AK. Numerical analysis of laminar natural convection in a quadrantal cavity with a solid adiabatic fin attached to the hot vertical wall. *J. Appl. Fluid Mech.* 2013 Oct 1;6(4):501-10.
11. Serrano-Arellano J, Xamán J, Álvarez G. Optimum ventilation based on the ventilation effectiveness for temperature and CO2 distribution in ventilated cavities. *Int. J. Heat Mass Transf.* 2013 Jul 1;62:9-21.
12. Bettaibi S, Kuznik F, Sediki E. Hybrid LBM-MRT model coupled with finite difference method for double-diffusive mixed convection in rectangular enclosure with insulated moving lid. *Physica A.* 2016 Feb 15;444:311-26.
13. R.A. Granger. Introduction to vortex dynamics,*V.Karman Institute Lecture Series*. 1986; 1:1-08
14. Tsitverblit N, Kit E. Numerical study of axisymmetric vortex breakdown in an annulus. *Acta Mech.*1996 Mar;118:79-95.
15. Bessaih R, Marty P, Kadja M. Numerical study of disk driven rotating MHD flow of a liquid metal in a cylindrical enclosure. *Acta Mech.* 1999 Sep; 135:153-67.
16. Bessaïh R, Boukhari A, Marty P. Magnetohydrodynamics stability of a rotating flow with heat transfer. *ICHMT.* 2009 Nov 1; 36(9):893-901.
17. Dash SC, Singh N. Stability boundaries for vortex breakdowns and boundaries between oscillatory and steady swirling flow in a cylindrical annulus with a top rotating lid. *J. Braz. Soc. Mech. Sci. & Eng* 2018 Jul;40(7):336.
18. Dash S, Singh N. Effects of partial heating of top rotating lid with axial temperature gradient on vortex breakdown in case of axisymmetric stratified lid driven swirling flow. *Yildiz Technical University Press, Istanbul, Turkey, J. Thermal Eng.* 2016 Jul 1;2:883-96.
19. Dash SC. Study of axisymmetric nature in 3-d swirling flow in a cylindrical annulus with a top rotating lid under the influence of axial temperature gradient or axial magnetic field. *J. thermal eng*. 2017 Nov 15; 3(6):1588-606.
20. Dash, S. and Singh, N. Analysis of axisymmetric lid driven swirling flow under magnetic field with an axial thin rod," *ASME, Applied Mechanics and Materials Conf., MacMat.* May 30–June 1, 2011, Chicago, IL, USA.
21. Dash SC. Incompressible confined swirling flow in a cylindrical cavity with rotating lid under the influence of axial temperature gradient or axial magnetic field (*Doctoral dissertation, IIT, Kharagpur)*, 2015.
22. Simitev RD. Double-diffusive convection in a rotating cylindrical annulus with conical caps. *Phys. Earth Planet. Inter.* 2011 Jun 1; 186(3-4):183-90.
23. Ghaffarpasand O. Characterization of unsteady double-diffusive mixed convection flow with Soret and Dufour effects in a square enclosure with top moving lid. *J. Heat Mass Transf. Res.* 2018 May 1;5(1):51-68.
24. Satheesh A, Mohan CG, Padmanathan P, Kumar AA. Effects of Joules heating and Soret number on double-diffusive mixed convection flow in an enclosed square cavity. *In Proceedings of INCOTHERM KIIT Thermo* 2020 2021 (pp. 209-223). Springer Singapore.
25. Chatterjee D, Halder P, Mondal S, Bhattacharjee S. Magnetoconvective transport in a vertical lid-driven cavity including a heat conducting square cylinder with Joule heating. *Numer. Heat Transf. A.* 2013 Dec 15;64(12):1050-71.

© STM Journals 2026. All Rights Reserved

26. Dash SC, Singh N. Influence of axial magnetic field on swirling flow and vortex breakdown zones in a cylindrical cavity with a rotating lid. *IJAM or Int. J. Appl. Mech*. 2019 Jul 28;11(06):1950054.
27. Dash SC, Singh N. Effect of a strong axial magnetic field on swirling flow in a cylindrical cavity with a top rotating lid. *Int. J. Mod. Phys. C.* 2019 Nov 4; 30(11):1950092.
28. Dash SC. MHD braking and joules heating effect in a rotating confined cylindrical cavity packed with liquid metal. *FME Transactions*. 2021 Apr 1;49(2):437-44.
29. Dash SC. CFD analysis of Joule heating effect in a confined axi-symmetric swilling flow under the influence of axial magnetic field. *IJCMSE.* 2021 Sep 28;10(03):2150010.
30. Sammouda M, Gueraoui K. MHD double diffusive convection of Al2O3-water nanofluid in a porous medium filled an annular space inside two vertical concentric cylinders with discrete heat flux. *J. Appl. Fluid Mech.* 2021 May 10;14(5):1459-68.
31. Dash SC. Effects of double diffusion and Soret effect on MHD braking of liquid metal packed between enclosed rotating cylindrical annulus. *IJMPC*. 2025;36(06):1-19.
32. Chorin, A. J. A numerical method for solving incompressible viscous flow prob-lems. *J. Comput. Phys*.1967; 2:2–26.
33. Peyret, R. and Taylor, D. Computational Methods for Fluid Flow, Berlin: *Springer-Verlag;* 1983.
34. Escudier MP (1984) Observations of the flow produced in a cylindrical container by a rotating endwall. Exp Fluids2(4):189–196

© STM Journals 2026. All Rights Reserved